Proceedings of the 4th International Conference on Mechatronics and Smart Systems
DOI: 10.54254/2755-2721/2026.34469

Design of Interlayer Adiabatic Tapered Couplers Based on Linearized Mapping of Energy Distribution

Shengjie Mao

School of Optical and Electronic Information, Huazhong University of Science and Technology, Wuhan, China
maoshengjie@hust.edu.cn

Abstract. Aiming at the problem of interlayer energy coupling of stacked waveguides in heterogeneous integrated photonic chips, this paper proposes an adiabatic taper design method based on the regulation of energy spatial distribution. Although the traditional linear taper has a simple layout, its energy distribution curve along the propagation direction exhibits nonlinear abrupt characteristics, and the slope near the phase matching point is excessively large, resulting in mode crosstalk and transmission oscillation. This study takes "linearization of energy distribution" as the design goal, establishes the mapping relationship between waveguide width and local energy distribution coefficient, uses rational functions to fit the target energy distribution curve, and then inverts the optimal taper geometry. Simulation results show that the designed taper significantly compresses the transition length of the phase matching region and effectively suppresses energy transmission fluctuations, and its comprehensive performance of mode-connection power transfer efficiency and stability is superior to that of traditional linear and parabolic tapers.

Keywords: Adiabatic Coupler, Heterogeneous Integration, Silicon Photonics, Energy Distribution Mapping, Tapered Waveguide

1. Introduction

In the field of silicon-based optoelectronics and heterogeneous integration technology, how to achieve efficient interlayer optical coupling between waveguides of different materials has always been a core challenge restricting system performance [1-5]. Silicon-based optoelectronics has become a key platform for optical interconnection, sensing and computing by virtue of CMOS-compatible processes, high refractive index contrast and large-scale integration capability. However, silicon itself has low luminous efficiency and is difficult to monolithically integrate with gain or nonlinear materials such as III-V semiconductors and lithium niobate directly. Heterogeneous integration technology stacks functional layers of different materials on the same chip through bonding or epitaxial growth, and at this time, the problem of low-loss transmission of optical signals between waveguides of different layers and different refractive indices must be solved. The efficiency of interlayer coupling directly determines the power consumption, crosstalk and process tolerance of the entire photonic chip [6-10].

© 2026 The Authors. This is an open access article distributed under the terms of the Creative Commons Attribution License 4.0 (https://creativecommons.org/licenses/by/4.0/).

DOI: 10.54254/2755-2721/2026.34469

To address this problem, Adiabatic Mode Evolution Structure (AMES) is favored for its wide bandwidth, low loss, insensitivity to wavelength and excellent process tolerance. A typical interlayer adiabatic coupler consists of two stacked waveguides with inversely tapered widths: one waveguide gradually narrows along the propagation direction, while the other gradually widens. In this process, optical power is smoothly transferred from one waveguide to another through mode hybridization and adiabatic conversion, avoiding the reflection loss caused by concentrated mode interference.

Traditional designs often directly adopt simple geometric functions to define the gradual profile of waveguide width, such as linear taper or parabolic taper. However, the limitation of such methods is that the linear change of waveguide width is not equivalent to the linear change of energy transmission rate. In fact, when the two waveguides are close to the phase matching point, the hybridization degree of the supermodes they form increases sharply, resulting in energy coupling mainly concentrated in a short interval around the matching point [11-14]. Therefore, the energy distribution curve along the propagation direction is not uniform, but presents an "S-shaped" characteristic with steep middle and gentle ends. Ignoring this physical law will lead to redundant coupler length or aggravated mode crosstalk, thereby weakening the overall performance of the device. This nonlinear distribution leads to an excessively large local energy change rate $\frac{dP}{dL}$ in the phase matching region, which is easy to excite higher-order modes or reverse coupling modes, manifested as severe oscillation of the Mode-Connection Power Transfer Efficiency (MCTE) curve and redundant device length [15, 16].

From the perspective of energy transmission dynamics, this paper proposes an inverse design idea: first define the desired energy distribution curve along the length, and then solve the corresponding waveguide width profile. This paper expects the energy distribution to be as close to linear as possible—that is, the power transfer ratio increases uniformly with the propagation distance to reduce the local slope. Although the ideal linear distribution will physically aggravate mode mismatch, this paper successfully obtains a tapered structure with both high transmission efficiency and smooth energy evolution through the compromise mapping of rational functions.

2. Energy distribution characteristics of linear taper

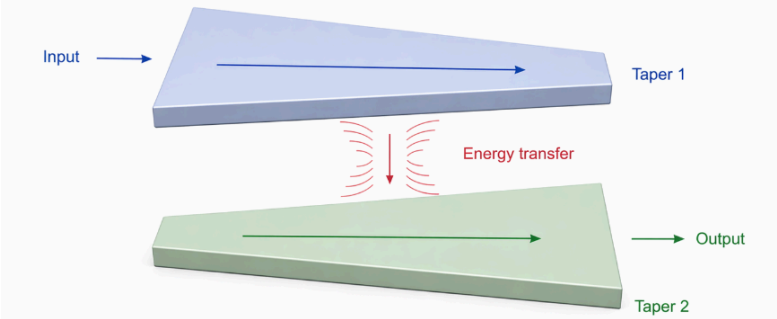

Figure 1. Schematic diagram of linear adiabatic taper

Taking a typical Si/SiN or Si/III-V stacked coupler as the research object (the total width of the upper and lower waveguides is constant, and the width changes are complementary). When adopting a linear width variation profile, this paper extracts the variation curve of the optical power distribution ratio in the two waveguides with the propagation length through Eigenmode Expansion (EME) scanning.

Its advantages are: direct layout generation without complex function fitting; meanwhile, at the input/output terminals far from the phase matching point, the change of waveguide width has little

DOI: 10.54254/2755-2721/2026.34469

disturbance to the mode field.

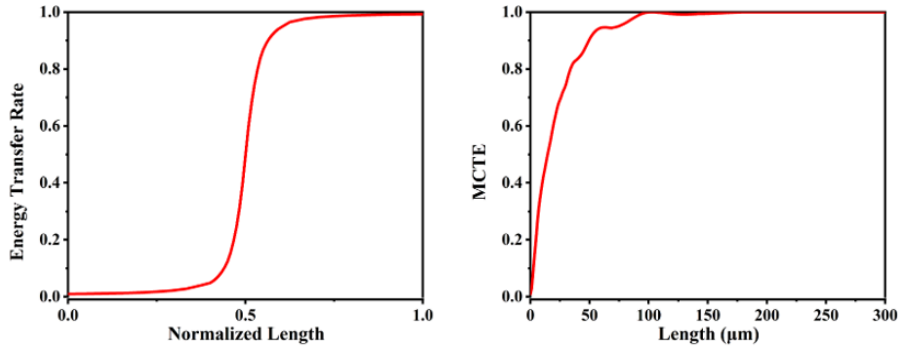

Figure 2. (a) Energy transfer curve of linear taper (b) MCTE curve

However, its disadvantages are also obvious: first, the nonlinear abrupt change of energy distribution. As shown in Figure 2(a), the energy transfer curve corresponding to the linear taper presents a typical S-shape. Near the phase matching point (i.e., the position where the power in the two waveguides accounts for 50% each), the slope $\frac{dP}{dL}$ of the curve reaches a peak, which means that in this narrow interval, the mode undergoes severe spatial reconstruction, and the effective refractive index change rate of the supermode is the largest, which is easy to couple to radiation modes or higher-order modes; meanwhile, the conduction speed of MCTE is slow, and the high slope of the local energy transfer curve directly leads to the oscillation behavior of MCTE with the total length. Suppressing the oscillation by extending the device requires a length cost several times higher, which is not conducive to high-density integration.

3. Design of novel taper based on rational function mapping

To solve the above problems, this paper proposes an "energy distribution priority" design strategy and introduces an energy distribution curve. Let P(z) be the power proportion in waveguide B, where $0 \leq P \leq 1$, and z is the normalized propagation distance. The ideal linear distribution is $P_{ideal}(z) = z$. However, the width profile solved under this target shows an approximate step at the phase matching point, resulting in severe fluctuations of the actual MCTE with the remaining length. The simulation results are shown in Figure 3.

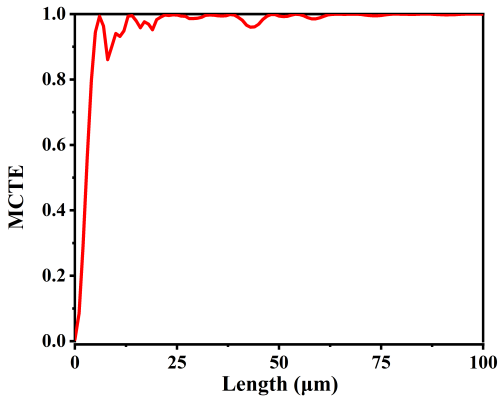

Figure 3. MCTE curve obtained by converting to ideal linear distribution

Therefore, this paper introduces a family of rational functions to modify the target distribution:

DOI: 10.54254/2755-2721/2026.34469

$$P_{target}(z) = \frac{z^m}{z^m + (1-z)^m} \tag{1}$$

where the parameter m controls the steepness of the middle section of the curve; it degenerates to linear when m=1; when m>1, the slope of the middle section increases, corresponding to more aggressive energy transfer. The optimal compromise between the "original linear taper distribution" and the "ideal linear distribution" can be found by selecting an appropriate m value.

Substitute the target distribution $P_{target}(z)$ into the mapping function to directly obtain the variation profile of waveguide width with propagation distance: $W(z) = g(P_{target}(z))$. The finally generated novel taper is named Rational Mapped Taper (RMT). This paper adopts a rational function with m=2 for mapping.

The specific simulation parameters are as follows:

Table 1. Simulation parameters

Parameter	Value
Taper length	1 μm (Normalizes)
Waveguide width	0.5 μm
Waveguide thickness	0.22 μm
Layer spacer	0.3 μm
Waveguide material	Si
Background material	SiO_2
Wavelength	1.55 μm
Excitation mode	Fundamental TE

The finally obtained energy transfer rate of RMT (i.e., $P(z) = \frac{z^2}{z^2+(1-z)^2}$) and MCTE curve are shown in Figure 4.

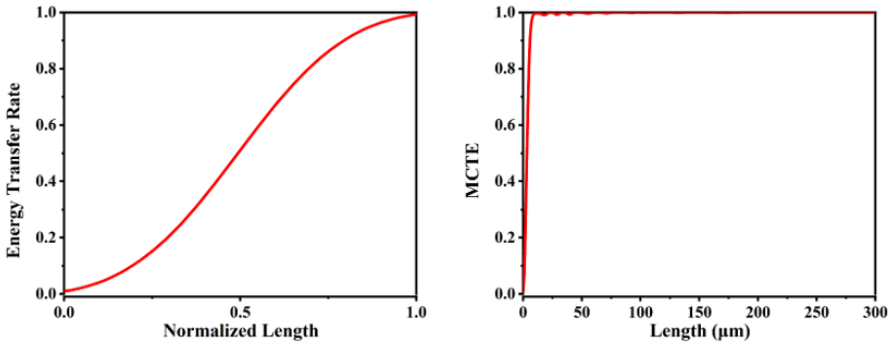

Figure 4. (a) Energy transfer curve of Rational Mapped Taper (RMT) (b) MCTE curve

3.1. Performance comparison and analysis

This paper conducts a comparative simulation of RMT with traditional linear taper and parabolic taper (wavelength 1550 nm, Si waveguide thickness 220 nm, width 500 nm, gap 300 nm). Among them, the parabolic shape is a taper form with lower loss and lower change in the mode-sensitive

DOI: 10.54254/2755-2721/2026.34469

region obtained in previous engineering optimizations. For the convenience of comparison and consideration of actual processes in this paper, the tapers all take a top width of 50 nm and a bottom width of 500 nm, which is intercepted as $y^2 = 0.06\left(x + \frac{1}{24}\right)(\mu m)$ in the normalized parabola.

The comparison of energy distribution curves of the three different tapers is as follows:

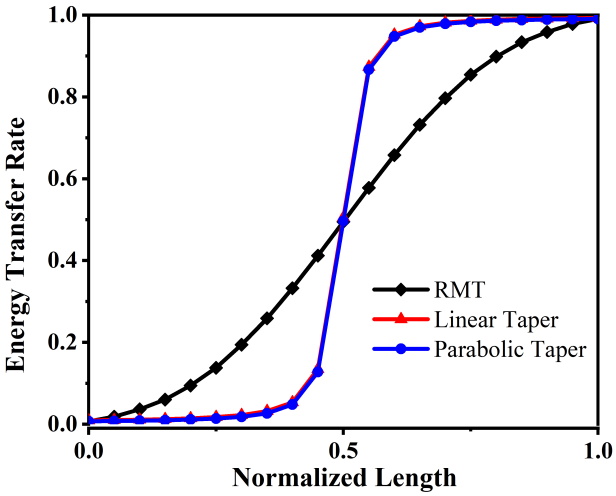

Figure 5. Comparison of energy transfer curves between RMT, linear taper and parabolic taper

Figure 5 shows the power distribution variation curves with length corresponding to the three designs. The distribution of linear taper presents a significant S-shape with the largest slope in the middle section; the nonlinearity of parabolic taper is still obvious, which is similar to the properties of linear taper, and both will introduce great oscillation and instability; the distribution curve of RMT is significantly straightened, and the local slope in the 40%~60% power interval is reduced by about 35%, which means the mode evolution is more gentle.

Comparison of MCTE variation with length:

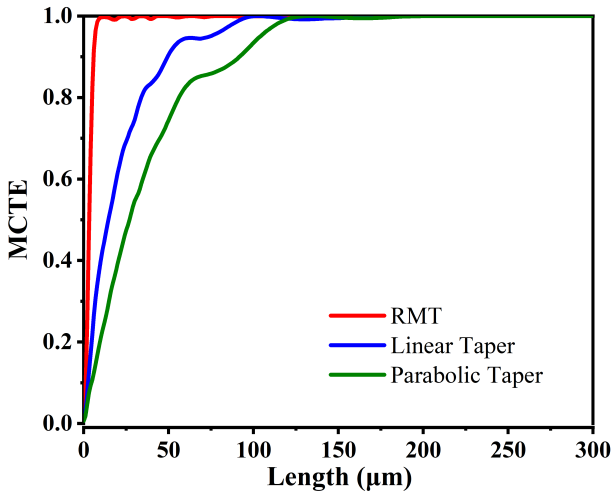

Figure 6. Comparison of MCTE curves between RMT, linear taper and parabolic taper

Figure 6 shows the scanning curves of MCTE of the three tapers with the total length L. RMT enters the high transmission efficiency region (>95%) at an extremely short length (5~6 μm), and the oscillation amplitude is significantly smaller than that of linear taper. When reaching 99% transmission efficiency, the length required by RMT is only 9 μm, which is about 90% shorter than

DOI: 10.54254/2755-2721/2026.34469

that of linear taper and about 92% shorter than that of parabolic taper. The envelope of the MCTE curve of RMT rises faster and fluctuates less, indicating that it has better robustness to process errors and wavelength drift.

3.2. Influence of lateral offset on performance

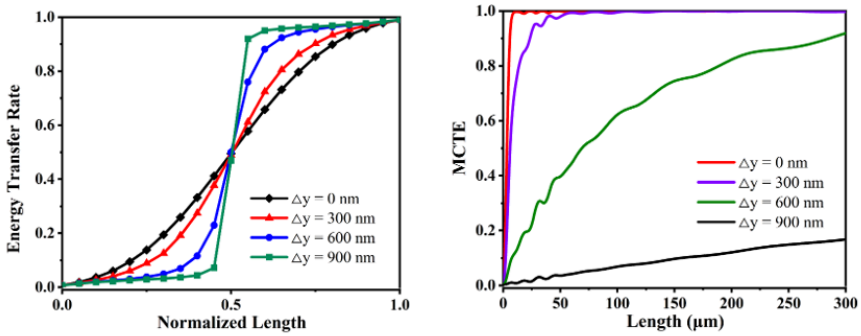

Figure 7. (a) Energy transfer curve of linear taper (b) MCTE curve

Figure 7 lists the influence of lateral (y-direction) offsets of 300/600/900 nm on the performance of RMT (energy transfer rate, MCTE) respectively. It can be easily seen from the figure that the lateral offset at a small scale has little influence on the performance of RMT, which further proves the robustness and stability of RMT to errors.

4. Conclusion

This paper re-examines the design problem of interlayer adiabatic couplers from the perspective of energy transmission dynamics. By distinguishing the "linear change of waveguide width" from the "linear change of energy distribution", this paper proposes an inverse taper design method (RMT) based on rational function mapping. This method transfers the design freedom from the geometric domain to the energy domain, allowing designers to directly regulate the distribution slope of power along the propagation direction. Simulation results show that RMT significantly reduces the energy change rate in the phase matching region while maintaining high MCTE, thus suppressing mode crosstalk and transmission oscillation. The design idea can be extended to any multi-layer waveguide heterogeneous integration scenario, providing a compact and stable coupling solution for 3D optical interconnection.

References

[1] Sherwood-Droz, N., & Lipson, M. (2011). Scalable 3D dense integration of photonics on bulk silicon. Optics express, 19(18), 17758-17765.

[2] Zhang, J., Chen, W., Zhang, T., Wang, F., Zeng, X., Zhang, X., ... & Wang, T. (2025). Multi-step-index fiber model and optimization for enhanced adiabatic and ultra-short tapering. Journal of Lightwave Technology, 43(17), 8344-8350.

[3] Pan, K., Meng, D., & Wang, Y. (2024). An ultra-broadband, and low loss 3-dB optical power splitter with curved adiabatic taper. Optics Communications, 569, 130729.

[4] Xia, Y., Huang, Y., Liu, M., Wang, J., Li, Z., Li, Y., ... & Xiang, C. (2025). 3D Silicon Nitride Waveguide Interposers for High-Density Scale-up Chiplet Interconnects. In 2025 European Conference on Optical Communications (ECOC) (pp. 1-4). IEEE.

[5] Xu, B., Huang, Y., Fang, Y., Wang, Z., Yu, S., & Xu, R. (2022). Recent progress of neuromorphic computing based on silicon photonics: Electronic–photonic Co-design, device, and architecture. In Photonics (Vol. 9, No. 10, p. 698).

DOI: 10.54254/2755-2721/2026.34469

MDPI.
[6] Zhai, S., Feng, J., Sun, X., Huang, Y., Zhou, L., He, J., ... & Zeng, H. (2019). Dual-Layer Cross-Coupled Tunable Resonator System in a Three-Dimensional Si3N4 Photonic Integration Platform. Journal of Lightwave Technology, 37(13), 3298-3304.
[7] Dhingra, N., Chen, Y. H., & Shenoy, V. (2024, March). Adiabatic tapers based on photonic inverse design. In Physics and Simulation of Optoelectronic Devices XXXII (Vol. 12880, pp. 143-149). SPIE.
[8] Zuo, G., Li, W., Yang, Z., Li, S., Qi, R., Huang, Y., & Xia, L. (2020). Double phase matching in MZI with antiresonant effect for optical fiber sensor application. Journal of Lightwave Technology, 39(2), 660-666.
[9] Charau, A. Y., Laurent, J., & Valier-Brasier, T. (2025). Adiabatic Lamb modes in 3D tapered waveguides: Cut-off effects and ZGV resonances. Ultrasonics, 155, 107733.
[10] Lee, E. S., Chun, K. W., Jin, J., Lee, S. S., & Oh, M. C. (2023). Monolithic integration of polymer waveguide phase modulators with silicon nitride waveguides using adiabatic transition tapers. Optics Express, 31(3), 4760-4769.
[11] Zuo, G., Hu, H., Li, S., Yang, Z., Chen, J., Huang, Y., ... & Xia, L. (2021). Iterative normalized cross-correlation method for absolute optical path difference demodulation of dual interferometers. Optics Express, 29(11), 16595-16610.
[12] Kudalippalliyalil, R., Chakraborty, T., Murphy, T. E., & Grutter, K. E. (2024). 3D self-aligning, polarization-independent fiber-to-chip couplers. In Optical Fiber Communication Conference (pp. M1J-1). Optica Publishing Group.
[13] Xu, Z., Du, Z., Lin, J., Xiao, P., & Wang, Y. (2025). Deep-subwavelength waveguide taper with adiabatic-like performance based on epsilon-near-zero materials. Optics Letters, 50(21), 6465-6468.
[14] Huang, Y., Shi, M., Yu, A., & Xia, L. (2023). Design of multifunctional all-optical logic gates based on photonic crystal waveguides. Applied optics, 62(3), 774-781.
[15] Anelli, F., Annunziato, A., Loconsole, A. M., Francione, V. V., Cozic, S., Poulain, S., & Prudenzano, F. (2024). Mid-infrared interferometry with non-adiabatic tapered ZBLAN optical fiber. Optics Express, 32(11), 18944-18957.
[16] Zhang, W., Ebert, M., Reynolds, J. D., Chen, B., Yan, X., Du, H., ... & Thomson, D. J. (2021). Buried 3D spot-size converters for silicon photonics. Optica, 8(8), 1102-1108.